ACS APPLIED MATERIALS & INTERFACES

Letter

www.acsami.org

DNA-Directed Gold Nanodimers with Tailored Ensemble Surface-Enhanced Raman Scattering Properties

Xiang Lan,[†,‡] Zhong Chen,[†,‡] Xuxing Lu,[‡] Gaole Dai,[†,‡] Weihai Ni,*[,‡] and Qiangbin Wang*[,†,‡]

[†]Division of Nanobiomedicine and [‡]i-Lab, Suzhou Institute of Nano-Tech and Nano-Bionics, Chinese Academy of Sciences, Suzhou 215123 China

Supporting Information

ABSTRACT: Gold nanodimers (GNDs) are assembled with high uniformity as ideal surface-enhanced Raman scattering (SERS) substrates through DNA-directed self-assembly of gold nanoparticles. The interparticle distance within GNDs is precisely tailored on the order of a few nanometers with changing the molecule length of DNA bridge. The ensemble SERS activity of monodispersed GNDs is then rationally engineered by modifying the structural parameters of GNDs including the particle size and interparticle distance. Theoretical studies on the level of single GND evidence the particle size- and interparticle-distance-dependent SERS effects, consistent with the ensemble averaged measurements.

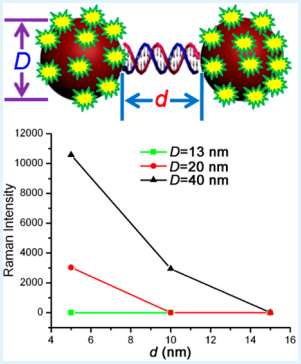

KEYWORDS: *gold nanoparticle, surface-enhanced Raman scattering, DNA self-assembly, nanostructure*

INTRODUCTION

Noble metal nanostructures support coherent oscillation of conduction electrons on the surface, termed localized surface plasmon resonance (LSPR), which is featured by enormous enhancement of local electric filed (hot-spot) in the nanogap junction of plasmon-coupled particles.[1−4] The enhanced electric field intensively amplifies the weak Raman signal by increasing the scattering cross-section of Raman active molecule in the vicinity of the hotspot.[5,6] This is known as electromagnetic mechanism in the effect of surface-enhanced Raman scattering (SERS). It is ideal that the Raman active molecules are excited similarly in SERS nanostructures, hence displaying narrow distribution of enhancement factor (EF).[7,8] Therefore, fabrication of the noble metal nanostructures with high uniformity and engineering of the surface plasmon coupling in a well-defined manner are critical.

So far, colloidal synthetic method and self-assembly technique have been widely exploited in preparation of noble metal nanostructures as SERS substrates by tuning the particle size, shape, interparticle distance and surface morphology, etc.[9−13] Most research has been focused on the study of SERS signal at the single molecule or nanoparticle level to reveal the individual response,[3−5,14] let alone the ensemble measurement of SERS behaviors due to the heterogeneity and scarcity of the desired SERS substrates, which induces largely variable hot spots and generates nonquantitative SERS signals. So far, few studies have reported monodispersed colloidal SERS nanostructures with well-engineered LSPR property by precisely varying the nanoparticle size and interparticle distance on the order of a few nanometers. The ensemble-averaged SERS signals from these highly uniform and rationally tailored SERS substrates in bulk solution, which have fundamental significance in their applications in biochemical systems,[15,16] have been rarely investigated as well.

In this work, we prepared monodispersed gold nanodimers (GNDs) by means of DNA-directed self assembly, where the interparticle distance is precisely defined by the nanoscale DNA molecule bridge. We then systematically investigated the particle size- and interparticle distance-dependance of the ensemble SERS properties by employing our DNA-directed GNDs as a model system, in which the Raman active molecule mercaptobenzoic acid (MBA) was immobilized on the surface of the well-defined GNDs. The ensemble SERS behaviours of the GNDs are well-engineered by tuning the constituent particle size and molecule length of DNA bridge. Theoretical studies on the level of single particle also evidence the same structure-dependent SERS activity of GNDs.

EXPERIMENTAL SECTION

Preparation of 13, 20, and 40 nm AuNPs and Surface Modification. Thirteen nanometer AuNPs were prepared following Fren's method.[17] $HAuCl_4$ aqueous solution (50 mL, 1 mM) was brought to boiling, then sodium citrate (5 mL, 1% w/v) was added under vigorous stirring. The solution was cooled slowly to room temperature after 15 min.

Received: September 16, 2013
Accepted: October 11, 2013
Published: October 11, 2013

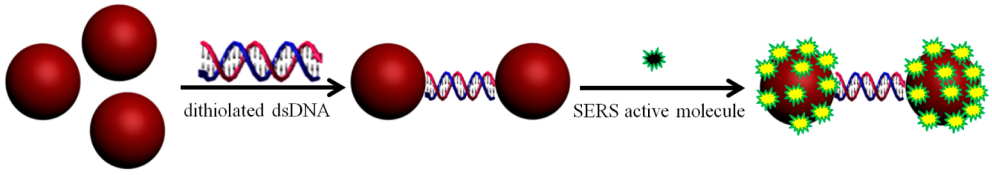

Figure 1. Schematic illustration of the fabrication of GNDs as SERS substrate, in which the particle size and interparticle distance can be finely tuned. The AuNPs are firstly bridged by dsDNA with dithiol group at both ends, the GNDs are coated with Raman active molecule (MBA) and then purified through gel electrophoresis.

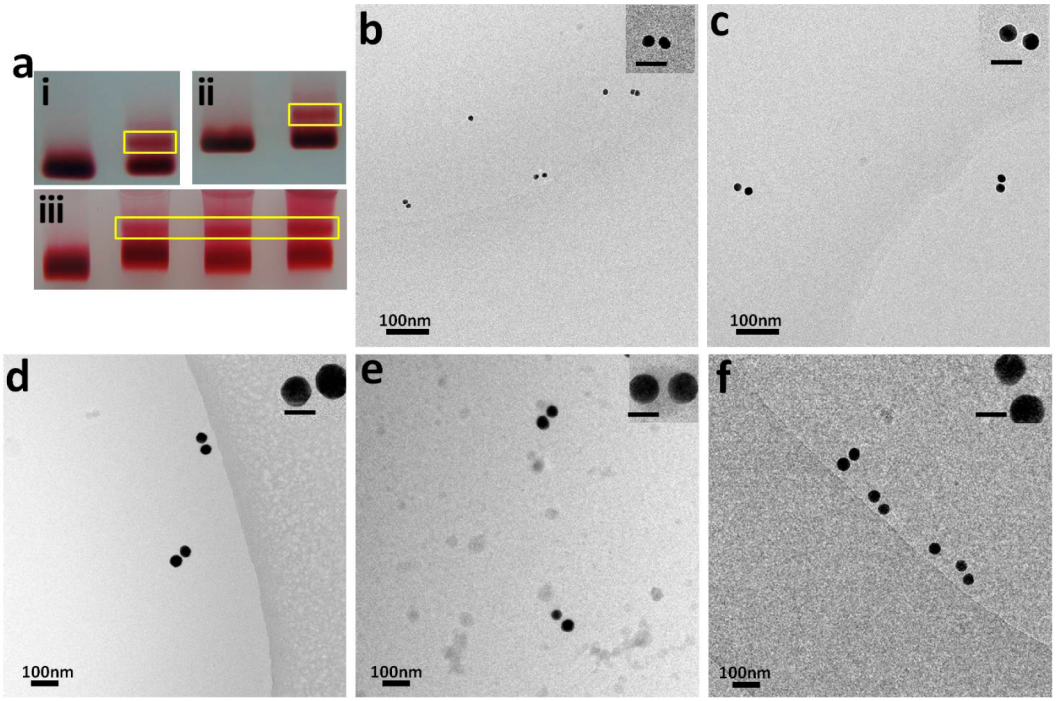

Figure 2. Characterization of GNDs. (a) Electrophoresis images of DNA-directed GNDs. (i) GND1; (ii) GND2; (iii) GND3, GND4, and GND5. (b–f) Cryo EM images of DNA-directed GNDs: (b) GND1; (c) GND2; (d) GND3; (e) GND4; (f) GND5. The scale bars in inset high-magnification images are 40 nm.

20 nm AuNPs were prepared using 13 nm AuNPs as seeds. Thirteen nanometer AuNP solution (50 mL, 2 nM) was placed in a 200 mL flask. Sodium citrate (980 μL, 1% w/v), $HAuCl_4$ solution (980 μL, 24.2 mM), and ascorbic acid (980 μL, 1% w/v) were added separately over 1 h. The mixture was heated to boiling and kept at that temperature for 30 min, and then cooled slowly to room temperature.

40 nm AuNPs were prepared using 20 nm AuNPs as seeds. 20 nm AuNP solution (50 mL, 2 nM) was placed in a 200 mL flask. Sodium citrate (9.5 mL, 1% w/v), $HAuCl_4$ solution (9.5 mL, 24.2 mM), and ascorbic acid (9.5 mL, 1% w/v) were added separately over 1 h. The mixture was heated to boiling and kept there for 30 min, and then the solution was cooled slowly to room temperature.

For surface modification of the AuNPs, excess of bis(*p*-sulfonatophenyl)-phenylphosphine (BSPP) was added to the as-prepared AuNPs solution to replace the citrate capping and enhance the stability of AuNPs against the salted buffer condition.

DNA Sequences. The sequences of DNA (from 5′ to 3′) used in this study for assembling GNDs are: P15, TGAGTCTCGTGGCAC-NH_2; P15c, GTGCCACGAGACTCA-NH_2; P30, GCATCCGGTCCAACTTGAGTCTCGTGGCAC-NH_2; P30c, GTGCCACGAGACTCAAG TTGGACCGGATGC-NH_2; P45, TGTGTACTAGGCCGAGCATCCGGTCCAACTTGAGT CTCGTGGCAC-NH_2; P45c, GTGCCACGAGACTCAAGTTGGACCGGATGCTCGGCCTA GTACACA-NH_2.

Assembly and Purification of GNDs. The amine-terminated DNA strand was further modified with thioctic acid following Yan's protocol[18] to enhance the interaction between AuNPs and DNA. Thioctic acid-terminated single-stranded DNA (ssDNA) was hybridized into double-stranded DNA (dsDNA), and the dsDNA was then conjugated to BSPP-coated AuNPs in aqueous buffer (0.5 × TBE, 50 mM NaCl). After incubation for 12 h, excessive mercaptobenzoic acid (MBA) was added to the reaction mixture. The reaction mixture was incubated for another 12 h. Lastly, The GNDs were separated from free AuNPs and other conjugates by 2% agarose gel electrophoresis. After gel separation, the target band sliced from gel was eluted in a dialysis membrane (8000–14000) through electrophoresis.

Characterization. Extinction spectra were acquired on a lambda 25 UV-Vis spectrometer (PerkinElmer). All samples were examined under a FEI Tecnai 20 TEM (operated at 200 kV) equipped with a Gatan UltraScan 894 CCD camera. Cryo-EM characterization was performed under Tecnai 20 TEM (operated at 200 kV) equipped with a Gatan 626 and Gatan

CT3500 low temperature sample holder. For SERS characterization, 100ul solution of GNDs covered with MBA SERS active molecules was placed in a plastic container under an objective (50×). Raman measurement was performed with excitation laser of 633 nm in wavelength. The measured SERS spectra were normalized by keeping the same concentration of MBA molecules per GND. The gold nanoparticle surface was fully covered by MBA, as the MBA molecules were in large excess to nanoparticles, thus, we tuned the concentration of GNDs in SERS measurement based on varying particle size with a GNDs1/GNDs2/GNDs3 concentration ratio of 9.47:4:1. The enhancement factor of electric field as a theoretical proof was calculated at the hot-spot in the nanojunction of GNDs. The particle size- and interparticle distance-dependent SERS property of GNDs was found much correlated with this electric-field enhancement.

RESULTS AND DISCUSSION

As shown in Figure 1, the GNDs are generated by bridging the single gold nanoparticles (AuNPs) with dsDNA molecule through dithiol groups at both ends. DNA linker is added directly to the BSPP-capped gold nanoparticles at equal molar ratio in 50 mM NaCl solution. Subsequently, the GNDs are fully covered by Raman active molecule (MBA) replacing the BSPP through addition of excess MBA into the GNDs in 0.5 × TBE buffer with 30 mM NaCl. The reaction mixture is incubated overnight. Owing to the strong binding between AuNPs and dithiolated DNA, the single thiol group of MBA has little influence on the stability of GNDs. The resultant GNDs are then purified by 2% agarose gel electrophoresis. In order to quantitatively understand the effect of particle size and interparticle distance on the SERS behavior of GNDs, the size of AuNP is varied from 13 nm to 20 nm and 40 nm, and the interparticle distance is tuned from 5 to 10 and 15 nm by changing the molecule length of DNA linker from 15 base pair (bp) to 30 bp and 45 bp (~0.34 nm/bp). In the current study, five kinds of GNDs are designed as 13 nm−13 nm AuNP with 5 nm separation (GND1), 20 nm−20 nm AuNP with 5 nm separation (GND2), 40 nm−40 nm AuNP with 5 nm separation (GND3), 40 nm−40 nm AuNP with 10 nm separation (GND4), and 40 nm−40 nm AuNP with 15 nm separation (GND5).

Figure 2a shows the electrophoresis images of the GNDs with free AuNPs as control. Obviously, the GNDs were obtained in a high purity after electrophoresis purification as evidenced by the two respective sharp bands of the free AuNPs and the assembled GNDs, which guarantees the ensemble-averaged measurement of the collective SERS behaviour of GNDs. Figure 2b−f of the Cryo EM images reveals the high purity of the obtained GNDs and the good agreement of experimental observation with our design, in which the size of AuNP and interparticle distance of the GNDs are precisely engineered. It is worth noting that, arising from different projection angles between the electron beam and the samples randomly oriented in the ice, the deviated 2D projections of GNDs are observed, which may not provide the correct interparticle distances.

As the surface plasmon resonance coupling within the GNDs is strongly affected by the particle size and interparticle distance, tuning these two parameters enables well manipulation of the resulting LSPR property and leads to tunable SERS response of the analyte molecule. Figure 3 shows the experimentally measured MBA SERS spectra of different

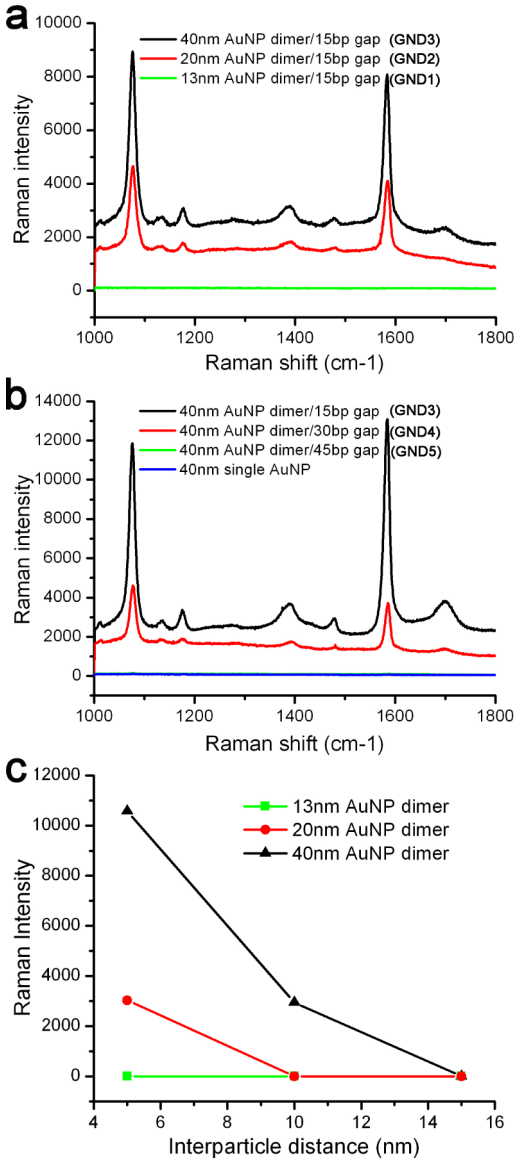

Figure 3. SERS properties of GNDs. (a) Experimental measurement of SERS spectra of GND1, GND2, and GND3, in which the AuNP size increases from 13 to 20 nm and 40 nm while keeping the interparticle distance of 5 nm. (b) Experimental measurement of SERS spectra of GND3, GND4, and GND5, in which the interparticle distance increases from 5 nm to 10 nm and 15 nm while keeping the AuNP size of 40 nm. (c) The measured MBA SERS intensities of different GNDs with background noise deducted.

GNDs. In a group of GND1, GND2, and GND3, the size of AuNP increases from 13 nm to 20 nm and 40 nm, while keeping the interparticle distance constant of 5 nm. As shown in Figure 3a, GND3 has the strongest SERS intensity, GND2 has the second strongest SERS intensity, and GND1 has no SERS signal. These results reveal that the AuNP size plays an important role in determining the SERS behavior. Increasing the interparticle distance from 5 to 10 and 15 nm with the AuNP size of 40 nm, the SERS intensities decrease dramatically as shown in Figure 3b, indicating the weakened plasmon coupling interaction within the GNDs. Our ensemble-measured SERS spectra of GNDs demonstrate the size and distance dependence of the SERS properties. It must be noted that the numbers of the SERS active molecule of MBA immobilized on

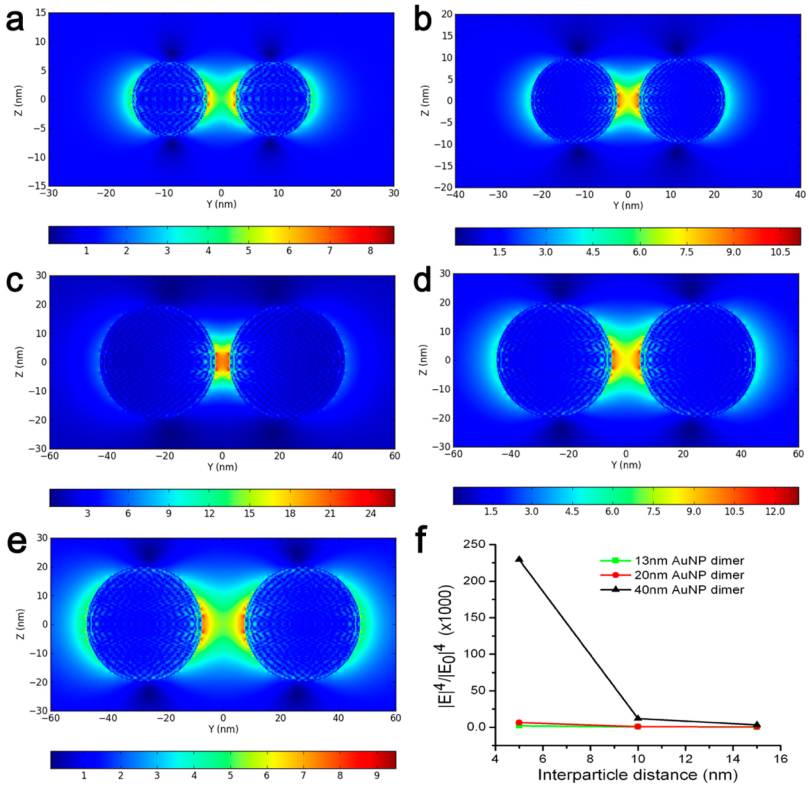

Figure 4. Calculated results for the GNDs. (a–e) Electric field enhancement profiles ($|E|/|E_0|$) of GND1, GND2, GND3, GND4, and GND5, respectively. (f) SERS enhancement factor, $|E|^4/|E_0|^4$, as a function of interparticle distance for the GNDs with AuNP sizes of 13, 20, and 40 nm.

the different sized AuNP surfaces have been normalized in this study, which guarantees the measured SERS intensity of GND1, GND2, and GND3 comparable.

Discrete dipole approximation (DDA) was performed to calculate the near-field enhancement from the GNDs. The DDA method, which is based on simulating the target with an array of interacting dipoles and solving their dipole moments in response to the local electric field, is a highly efficient and flexible technique for calculating the scattering and absorption of particles with arbitrary shapes and compositions.[19−23] In this calculation, the widely used DDA code, DDSCAT (version 7.1),[20] is employed. We considered that the GND was illuminated by an incident light with a wavelength of 630 nm. The polarization of the incident light was set along the dimer's axis. The refractive index of the ambient medium was set as 1.33, and the dielectric constant of Au was adapted from the previous report.[24]

Figure 4 represents the calculated E-field enhancement profile ($|E|/|E_0|$) in a plane perpendicular to the incidence direction. The calculation results reveal that the E-field enhancement reaches the maximum in the middle region of the gap, suggesting the strong coupling between the two proximal AuNPs. It also clearly indicates that the EF has a strong dependence on the geometric parameters of the GNDs. For the samples of GND3, GND4, and GND5 with the AuNP size of 40 nm, the E-field EF increases rapidly from 7.8 to 23.4 as the interparticle distance decreases from 15 nm to 5 nm. Meanwhile, the size of AuNP also plays an important role in the calculation. When the AuNP size is reduced from 40 to 13 nm with a constant interparticle distance of 5 nm, the E-field EF decreases from 23.4 to 8.5. These results are highly consistent with the experimental measurement as shown in Figure 3.

CONCLUSION

In conclusion, we have successfully fabricated a series of GNDs with high purity through DNA-directed self-assembly of AuNPs. Varying the size of employed AuNPs and the length of DNA linker molecule allows us precise tuning of the size and interparticle distance of the obtained GNDs, thus engineering the SERS properties. The experimentally measured ensemble SERS activities of GNDs exhibit particle size- and interparticle distance-dependent characteristics. Theoretical calculation on single GND level further verifies the impact of such two structural parameters on the resultant SERS properties of GND. The experimental SERS result of the ensemble GNDs matches very well with that of the calculation of a single GND, illustrating the power of the DNA-directed self-assembly in "bottom-up" fabrication of SERS substrates, and quantitative understanding of the effects of AuNP size and interparticle distance on the SERS behaviors will be suggestive for optimizing the future SERS substrate design.

ASSOCIATED CONTENT

Supporting Information

Additional figures (PDF). This material is available free of charge via the Internet at http://pubs.acs.org.

AUTHOR INFORMATION

Corresponding Authors

*E-mail: qbwang2008@sinano.ac.cn.
*E-mail: whni2012@sinano.ac.cn.

Notes

The authors declare no competing financial interest.

■ ACKNOWLEDGMENTS

We acknowledge funding by Chinese Academy of Sciences "Bairen Ji Hua" program, National Natural Science Foundation of China (Grant 91023038), Natural Science Foundation of Jiangsu Province (Grant BK2012007), and the CAS/SAFEA International Partnership Program for Creative Research Teams.

■ REFERENCES

(1) Camden, J. P.; Dieringer, J. A.; Zhao, J.; Van Duyne, R. P. *Acc. Chem. Res.* **2008**, *41*, 1653−1661.
(2) Osberg, K. D.; Rycenga, M.; Harris, N.; Schmucker, A. L.; Langille, M. R.; Schatz, G. C.; Mirkin, C. A. *Nano Lett.* **2012**, *12*, 3828−2832.
(3) Alexander, K. D.; Skinner, K.; Zhang, S.; Wei, H.; Lopez, R. *Nano Lett.* **2010**, *10*, 4488−4493.
(4) Wustholz, K. L.; Henry, A.-I.; McMahon, J. M.; Freeman, R. G.; Valley, N.; Piotti, M. E.; Natan, M. J.; Schatz, G. C.; Van Duyne, R. P. *J. Am. Chem. Soc.* **2010**, *132*, 10903−10910.
(5) Rycenga, M.; Camargo, P. H. C.; Li, W.; Moran, C. H.; Xia, Y. *J. Phys. Chem. Lett.* **2010**, *1*, 696−703.
(6) Nie, S.; Emory, S. R. *Science* **1997**, *275*, 1102−1106.
(7) Chen, G.; Wang, Y.; Yang, M.; Xu, J.; Goh, S. J.; Pan, M.; Chen, H. *J. Am. Chem. Soc.* **2010**, *132*, 3644−3645.
(8) Lim, D.-K.; Jeon, K.-S.; Hwang, J.-H.; Kim, H.; Kwon, S.; Suh, Y. D.; Nam, J.-M. *Nat. Nanotechnol.* **2011**, *6*, 452−460.
(9) Fang, J.; Du, S.; Lebedkin, S.; Li, Z.; Kruk, R.; Kappes, M.; Hahn, H. *Nano Lett.* **2010**, *10*, 5006−5013.
(10) Mulvihill, M. J.; Ling, X. Y.; Henzie, J.; Yang, P. *J. Am. Chem. Soc.* **2010**, *132*, 268−274.
(11) Tyler, T. P.; Henry, A.-I.; Van Duyne, R. P.; Hersam, M. C. *J. Phys. Chem. Lett.* **2011**, *2*, 218−222.
(12) Xie, J.; Zhang, Q.; Lee, J. Y.; Wang, D. I. C. *ACS Nano* **2008**, *2*, 2473−2480.
(13) Ahamad, N.; Ianoul, A. *J. Phys. Chem. C* **2011**, *115*, 3587−3594.
(14) Wei, H.; Hao, F.; Huang, Y.; Wang, W.; Nordlander, P.; Xu, H. *Nano Lett.* **2008**, *8*, 2497−2502.
(15) Wang, Y.; Yan, B.; Chen, L. *Chem. Rev.* **2013**, *113*, 1391−1428.
(16) Song, J.; Zhou, J.; Duan, H. *J. Am. Chem. Soc.* **2012**, *134*, 13458−13469.
(17) Frens., G. *Nature* **1973**, *241*, 20−22.
(18) Sharma, J.; Chhabra, R.; Andersen, C. S.; Gothelf, K. V.; Yan, H.; Liu, Y. *J. Am. Chem. Soc.* **2008**, *130*, 7820−7821.
(19) Draine, B. T. *Astrophys. J.* **1988**, *333*, 848−872.
(20) Draine, B. T.; Flatau, P. J. *J. Opt. Soc. Am. A* **1994**, *11*, 1491−1499.
(21) Draine, B. T.; Flatau, P. J. *J. Opt. Soc. Am. A* **2008**, *25*, 2693−2703.
(22) Yurkin, M. A.; Hoekstra, A. G. *J. Quant. Spectrosc. Radiat. Transfer* **2011**, *112*, 2234−2247.
(23) Mc Donald, J.; Golden, A.; Jennings, S. G. *Int. J. High Perform. Comput. Appl.* **2009**, *23*, 42−61.
(24) Johnson, P. B.; Christy, R. W. *Phys. Rev. B* **1972**, *6*, 4370−4379.